Bioelectrochemistry 132 (2020) 107418

Contents lists available at ScienceDirect

Bioelectrochemistry

journal homepage: www.elsevier.com/locate/bioelechem

Electrocatalytic nanostructured ferric tannate as platform for enzyme conjugation: Electrochemical determination of phenolic compounds

Massimiliano Magro [a], Davide Baratella [a], Veronica Colò [a], Francesca Vallese [b], Carlo Nicoletto [c], Silvia Santagata [c], Paolo Sambo [c], Simone Molinari [d], Gabriella Salviulo [d], Andrea Venerando [a], Caroline R. Basso [e], Valber A. Pedrosa [e], Fabio Vianello [a,*]

[a] Department of Comparative Biomedicine and Food Science, University of Padua, Agripolis – Viale dell'Università 16, 35020 Legnaro, PD, Italy
[b] Department of Biomedical Sciences, University of Padova, Via Ugo Bassi 58/B, Padova 35131, Italy
[c] Department of Agronomy, Food, Natural Resources, Animals and the Environment, University of Padua, Viale dell'Università 16, Legnaro 35020, PD, Italy
[d] Department of Geosciences, University of Padua, Via Gradenigo 6, 35131 Padova, Italy
[e] Institute of Bioscience, Department of Chemistry and Biochemistry, UNESP, Botucatu, SP, Brazil

ARTICLE INFO

Article history:
Received 29 August 2019
Received in revised form 15 November 2019
Accepted 17 November 2019
Available online 2 December 2019

Keywords:
Biosensor
Laccase
Tannic acid
Magnetic nanoparticles
Enzyme immobilization
Phenolic determination
Hybrid nanomaterials

ABSTRACT

A shell of nanostructured ferric tannates was spontaneously developed on the surface of naked maghemite nanoparticles (SAMNs, the core) by a simple wet reaction with tannic acid (TA). The as obtained core–shell nanomaterial (SAMN@TA) displays specific electrocatalytic and surface properties, which significantly differ from parent maghemite. Thanks to the known proclivity of TA to interact with proteins, SAMN@TA was proposed as a support for the direct immobilization of an enzyme. A ternary functional nanobioconjugate (SAMN@TA@*TvL*) was successfully self-assembled by incubating laccase from *Trametes versicolor* (*TvL*) and SAMN@TA. The SAMN@TA@*TvL* hybrid was kinetically characterized with respect to the native enzyme and applied for building an easy-to-use analytical device for the detection of polyphenols. The electrochemical biosensor allowed the determination of polyphenols by square wave voltammetry in mixed water-methanol solutions. The system sensitivity was 868.9 ± 1.9nA μM^{-1}, the LOD was 81 nM and the linearity range was comprised between 100 nM and 10 μM. The proposed approach was successfully applied to detect phenolics in blueberry extracts as real samples. Results suggest that SAMN@TA could be a promising, low cost and versatile tool for the creation of nano-bio-conjugates aimed at the development of new electrochemical sensing platforms.

1. Introduction

The conjugation of biological molecules to solid electrodes is commonly proposed for the development of biosensing devices [1]. Nevertheless, enzyme stability and activity should be maintained upon binding and the immobilization process should not affect the analytical performances of the electrode. In this scenario, nanomaterials are increasingly proposed as solid supports for electroanalytical applications and a number of core-shell nanostructures can be ideally obtained by the combination of enzymes and different nanoparticles [2]. In addition, a wide choice of chemical approaches can be employed for macromolecule immobilization purposes including physical absorption and electrostatic interactions as well as covalent immobilizations (e.g. ether, thio-ether, amide or carbamate bonds) [3–5]. Notwithstanding, enzyme conjugation to nanomaterials remains object of intense study as the immobilization strategy strongly influences the final hybrid properties with hardly predictable consequences on the catalytic performances [6]. In fact, the binding process can lead to drastic structural alterations of the enzyme, hence affecting the catalytic properties [7–9]. In the worst situation, the conjugation to a solid surface could induce protein denaturation and, consequently, the complete loss of the biological activity [10]. Thus, the preservation of catalytic activity of an enzyme is not a trivial task and is of crucial importance for providing effective nano-bio-conjugates with exploitable biological properties [11,12]. As an example, novel nanoparticles with peculiar surface properties were proposed as versatile building blocks to facilitate the immobilization process of biomolecules via self-assembly aimed at guaranteeing the

Abbreviations: BSA, bovine serum albumin; DLS, dynamic light scattering; FRAP, fluorescence recovery after photobleaching; SAMN, surface active maghemite nanoparticle; TA, tannic acid; TEM, transmission electron microscopy; *TvL*, *Trametes versicolor Laccase*.

* Corresponding author.
E-mail address: fabio.vianello@unipd.it (F. Vianello).

https://doi.org/10.1016/j.bioelechem.2019.107418
1567-5394/

preservation of enzyme activity, without requiring any chemical procedure or the use of additional coupling agents [13–15].

Tannic acid (TA) is known to interact with proteins forming soluble and insoluble complexes [16], and was already used as surface modifier for the functional coating on iron oxide nanoparticles (surface active maghemite nanoparticles, SAMNs) where the resulting core-shell hybrid (SAMN@TA) resulted one of the most robust tannic acid conjugate to date [17]. This was due to the drastic reorganization of the crystalline structure of the nanoparticle at the boundary with the solvent, leading to the formation a complex ferric tannate network and endowing novel electrocatalytic properties [18]. Herein, the immobilization of an enzyme (laccase from *Trametes versicolor*, *TvL*) was carried out for the first time using SAMN@TA as solid support by self-assembly in water, leading to a SAMN@TA@*TvL* ternary hybrid combining the magnetic properties of maghemite nanoparticles and the electrocatalytic features of ferric tannate, still maintaining the biological activity of laccase.

Laccases (benzendiol:oxygen oxidoreductases; EC 1.10.3.2) are multi-copper oxidases, widely distributed among plant and fungal species [19]. Their physiological role has not been completely understood and probably depends on the specific species. They generally present a broad substrate specificity, and can oxidize phenols, anilines, benzenthiols and phenothiazines [20], being molecular oxygen the electron acceptor of a four electron process leading to water production as final reduction product [21]. Among fungal laccases, a high variability was observed in the polymorphism, induction mechanism, chemical-physical properties and catalytic activity [22–24].

Various laccase based biosensors were already applied for the detection of phenolic compounds in plant extracts [25–28]. Alternatively, tyrosinases were also used as bioelements for this purpose [29,30].

Phenolic substances constitute a large group of natural compounds, widely distributed in fruits and vegetables. Many of them are derived from the processing of vegetal products and in a variety of industrial processes, e.g. in the manufacturing of plastics, paper, dyes, drugs, pesticides and antioxidants [31–33]. It should be considered that some phenolics are pollutants of concern, being highly toxic [34]. For these reasons, their determination is of great importance and rapid and sensitive procedures for their detection are of growing interest.

The present work reports on the preparation and characterization of the SAMN@TA@*TvL* ternary hybrid, and on its application for the development of an immersion probe amperometric biosensor for polyphenols detection. Noteworthy, the final biosensor configuration was obtained by simply immobilizing SAMN@TA@*TvL* on a commercially available gold electrode by means of an external magnet.

The here presented system, besides being a cost-effective option for the determination of polyphenols, envisages the potential of SAMN@TA as a platform for creating novel enzymatically active and magnetically drivable nano-bio-conjugates.

2. Experimental

2.1. Chemicals

All reagents were of the highest commercially available purity and were used without further purification processes. Preliminary kinetic measurements were carried out in Britton-Robinson buffer, consisting of a mixture of 0.033 M H_3BO_3, 0.033 M H_3PO_4 and 0.033 M acetic acid, set at the desired pH with 1 M NaOH. Doubly distilled water was used. Final measurements were carried out in citrate buffer at optimized pH (pH 5.0). *TvL* was from Sigma-Aldrich (Italy) and purified by FPLC using a Superdex 200–10/300 column, a flow rate of 0.5–1.0 mL min^{-1} and 0.25 M NaCl in citrate buffer at pH 6.0 as carrier. Enzyme purity was checked by SDS-PAGE and it was >90%, after staining with Coomassie Brilliant Blue from Serva (Heidelberg, Germany). All other reagents were from Sigma-Aldrich (Italy).

2.2. Instrumentation

Optical spectroscopy measurements were performed by a Cary 50 spectrophotometer (Varian Inc., Palo Alto, CA, USA) in quartz cuvettes (1 cm p.l.). Transmission electron microscopy (TEM) images were acquired by a JEOL 2010 microscope operating at 200 kV with a point-to-point resolution of 1.9 Å. Before measurement, ethanol suspensions of SAMN@TA and SAMN@TA@*TvL* were treated by ultrasound for 5 min. A drop of the dilute suspension was placed onto a holey-carbon film supported by a copper-mesh TEM grid and air-dried at room temperature. A series of Nd-Fe-B magnets (N35, 263–287 kJ/m^3 BH, 1170–1210 mT flux density by Powermagnet – Germany) was used for all the nanoparticles separation procedures as well as for immobilization of the magnetic nanomaterial on the electrode (see paragraph *2.10. Electrochemical measurements* and paragraph *3.4. Development of a polyphenol biosensor*).

2.3. Real sample preparation

Fresh blueberry samples (1.0 g) obtained from a local market were homogenized by an Ultra Turrax T 25 digital homogenizer (IKA®-Werke GmbH & Co. Germany) for 30 s in 20 mL methanol. The as-obtained homogenate was filtered and stored at −80 °C until use.

2.4. Determination of polyphenols by spectrophotometry

Polyphenol concentration, expressed as hydroquinone concentration, was determined by the FRAP and Folin-Ciocalteau methods [35,36]. Each measurement was performed in triplicate.

2.5. Determination of polyphenols by HPLC

Polyphenols (quercitin-3-gal, quercitin, kaempferol, delfinidin-3-glu, cyanidin-3-glu, petunidin-3-glu, malvidin-3-glu, catechin, epicatechin, gallic acid, hydroxybenzoic acid, chlorogenic acid, caffeic acid, coumaric acid, ferulic acid, cinnamic acid) were separated and quantified using an HPLC equipped with a diode array detector. The liquid chromatography apparatus utilized for the analyses was a Jasco X-LC system consisting of a model PU-2080 pump, a model MD-2015 multiwavelength detector, a model AS-2055 autosampler, and a model CO-2060 column oven. ChromNAV chromatography data system was used as analytical software. The separation was obtained on a Tracer Extrasil ODS2 (5 mm, 250 6 45 mm – Teknokroma) operating at 35 °C. The flow rate was set at 1 mL min^{-1}. The mobile phase consisted of 0.1% formic acid (A) and methanol (B). All standards were dissolved in 50% methanol and the calibration curves were generated with standards at concentrations ranging from 0.06 to 60 mg L^{-1}.

2.6. Kinetic characterization of native and immobilized TvL

The catalytic activities of *TvL* was studied using 1,2-dihydroxybenzene, 1,3-dihydroxy-benzene and 1,4-dihydroxy-benzene as substrates. Enzyme activity measurements were carried out in 33 mM Britton Robinson buffer, pH 2.5–7.0 [37], and the pH was adjusted by additions of 1.0 M NaOH stock solution. Enzyme activity was measured by spectrophotometry, monitoring the rate of formation of 1,4-benzoquinone from 1,4-dihydroxy-benzene ($\varepsilon_{245nm} = 2.2 \times 10^4$ M^{-1} cm^{-1}) and the disappearance the substrate

in the case of 1,2-dihydroxy-benzene ($\varepsilon_{275nm} = 2.4 \times 10^3$ M^{-1} cm^{-1}). Enzyme activity was also followed by measuring oxygen consumption by a Yellow Springs oxygen electrode during substrate oxidation. Measurements were carried out in a 4.5 mL gas tight cell under continuous agitation at room temperature. The stoichiometric ratio, $\Delta[S]/\Delta[O_2]$, was calculated by injection of known amount of substrates ($\Delta[S]$) in the oxygraphic cell and measuring the decrease of O_2 concentration ($\Delta[O_2]$), being $[S] \ll [O_2]$. Enzyme activity toward 1,3-dihydroxy-benzene was measured only by oxygraphy. Enzyme catalytic parameters were obtained from initial rate of substrate oxidation measured within the first 5 min from substrate addition to the reaction solution. All measurements were carried out at room temperature (22 ± 1 °C) in the presence of 0.1 mM EDTA. Three replicates were performed to calculate the kinetic parameters.

2.7. Protein determination

Laccase concentration was determined according to the Bradford procedure [38], using bovine serum albumin for calibration.

2.8. Preparation of the SAMN@TA@TvL hybrid by self-assembly

The SAMN@TA core-shell nanostructure was prepared as already described [18]. Tannins are known to interact with proteins. In particular, tannin-protein complexes are normally formed by hydrogen bonds and hydrophobic interactions [39]. Thus, the SAMN@TA complex was used for the immobilization of the laccase from *Trametes versicolor*.

Preliminarly The suspension of SAMN@TA was prepared by sonicating a weighted amount of SAMN@TA powder in a known water volume. The suspension was stable in water for months. Thus, this mother suspension was used to obtain all other suspensions by dilution.

The immobilization of *TvL* on SAMN@TA was carried out by a simple self-assembly in water under end-over-end mixing at 4.0 °C. In this view, it is important to mention that the process was performed in water as saline solutions could destabilize colloidal suspensions of nanomaterials. [40]. Loosely bound enzyme was removed by repeated washing cycles with the aid of an external magnet. After the incubation period, nanoparticles were separated by the application of an external magnet and the presence of the biomolecule in the supernatant was checked by spectrophotometric assays (by Bradford colorimetric method and/or enzymatic activity). After three washing cycles, the activity of the immobilized enzyme was constant and no detectable enzyme release was observed in the solution (residual activity in the washing buffer was less than 1%).

In order to appreciate the spontaneous evolution of the system into a nanobioconjugate, SAMN@TA suspensions, spanning from 0.2 to 1.5 mg mL^{-1} were incubated in the presence of a constant enzyme concentration (2.5 μg mL^{-1}). After 1 h incubation, the nanomaterial was recovered from the aqueous milieu by the application of an external magnet. The measurement of the enzymatic activity under substrate (1,4-dihydroxybenzene) saturation conditions was used to assess the concentration of unbound *TvL* in solution after the magnetic removal. According to enzyme activity measurements, native *TvL* progressively disappeared from the solution as a function of SAMN@TA concentration roughly following an exponential decay (see Fig. 1). Native *TvL* in solution was completely bound on nanoparticles at around 0.5 mg mL^{-1} SAMNs.

In order to maximize the surface concentration of the enzyme on the final hybrid, the incubation was performed using 20 μg mL^{-1} *TvL* and 0.5 mg mL^{-1} SAMN@TA. At the end of the incubation, the enzyme in solution resulted of 11.5 μg mL^{-1}, corresponding to 23 mg bound laccase g^{-1} SAMN. The quantification

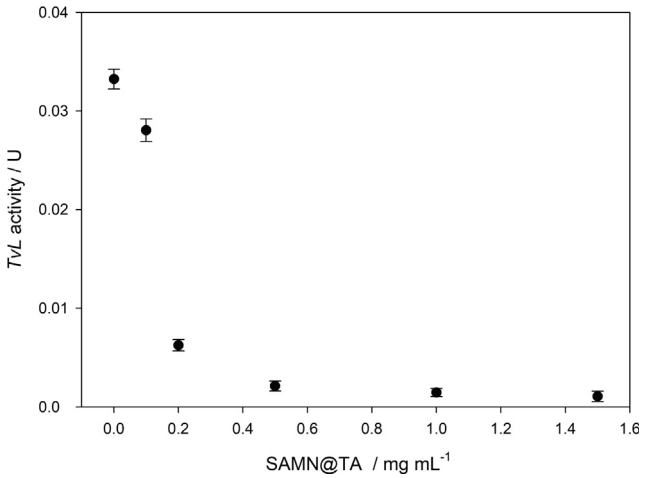

Fig. 1. Sequestration of *TvL* by SAMN@TA. The phenomenon was studied by measuring the enzymatic activity on 1,4-dihydroxybenzene as substrate following the production of 1,4-benzoquinone by spectrophotometry at λ = 245 nm. Measurements were carried out in 50 mM citrate buffer, pH 5.0, containing of 0.1 mM EDTA, in the presence of 2.5 μg mL^{-1} *TvL*, at room temperature (22 ± 1 °C).

of the immobilized enzyme was also performed using the Bradford method, using a calibration curve built with bovine serum albumin (BSA). In this case, the mass ratio of bound laccase on SAMN@TA was 24 mg g^{-1} SAMN, in very good agreement with the enzyme activity assay. Therefore, the calculated immobilization yield resulted 58.8 ± 1.3%.

2.9. Dynamic light scattering (DLS) measurements

DLS measurements, namely zeta potential and size distribution, of the SAMN@TA and SAMN@TA@*TvL* hybrids were measured by a Zetasizer Nano particle analyser ZEN3600 (Malvern Instruments, UK) in water at pH = 7.0, at T = 22 °C. Statistical analysis of the size distribution was obtained by using a lognormal function. All measurements were carried out at least in triplicate.

2.10. Electrochemical measurements

Electrochemical experiments were carried out by a computer-controlled electrochemical system (Autolab PGSTAT 12, Eco-Chemie, The Netherlands). Gold electrodes were kindly provided by Tectronik s.r.l. (Italy). They were constituted of two gold working electrodes (W1 and W2) and a pseudo-reference gold counter-electrode (RE-CE). The working electrode presented a diameter of 2 mm (see Fig. 2).

The SAMN@TA@*TvL* was magnetically immobilized on W1 surface and W2 was used as control electrode (see Fig. 2).

SAMN@TA, SAMN@TA@*TvL* modified gold electrodes as well as unmodified gold electrode were placed in an electrochemical cell (30 mL) containing 50 mM citrate buffer, containing 0.1 M KNO_3, and connected to the potentiostat. Square wave experiments were carried out using conventional counter (Pt) and reference (SCE) electrodes. Electrochemical measurements were carried out under continuous stirring at constant temperature (22.0 ± 0.2 °C). All experiments were repeated at least five times. The limit of detection (LOD) was calculated according to Miller and Miller [41].

3. Results and discussion

3.1. Characterization of the SAMN@TA@TvL hybrid

The SAMN@TA complex and the enzyme nanoconjugate (SAMN@TA@*Tvl*) were characterized by dynamic light scattering

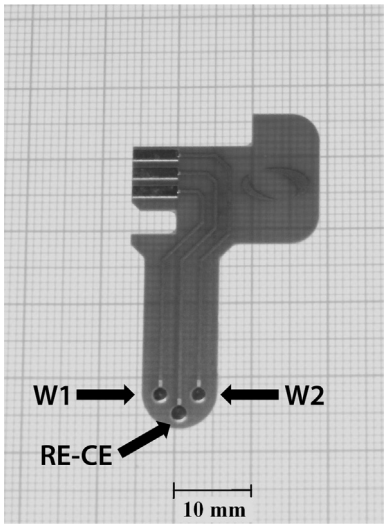

Fig. 2. Photographic image representing the electrode used for the development of the biosensor.

(DLS) and zeta potential (ζ) measurements. The hydrodymamic size of SAMN@TA and of SAMN@TA@*TvL* complexes, determined by DLS measurements, were 309.24 ± 6.08 nm, and 328.18 ± 2.27 nm, respectively (see Fig. 3 a and b). The measurements of the zeta-potential at room temperature and at pH = 7.0 showed that the enzyme immobilization was accompanied by a substantial increase of ζ, in term of absolute value, from –23.6 ± 9.0 mV for SAMN@TA (conductivity 0.0139 mS cm^{-1} in water at 22 °C) to −34.5 ± 8.2 mV for SAMN@TA@*TvL* (conductivity 0.1533 mS cm^{-1} in water at 22 °C). These results, besides witnessing the enzyme binding occurrence, indicate that both aqueous suspensions of SAMN@TA and SAMN@TA@*TvL* can be considered as stable accordingly to the scale reported by Patel and Agrawal [42].

Moreover, the SAMN@TA@*TvL* ternary hybrid was characterized by transmission electron microscopy (TEM). The development of core-shell nanostructures can be appreciated by observing the morphology of the material, actually consisting in crystalline spherical objects enveloped in a less electron-dense organic coverage (see Fig. 3c and d). In particular, the presence of a double layer around the core can be distinguished and can be attributed to an inner shell of ferric tannates and an outer shell attributable to the immobilized enzyme (see Fig. 3d).

The FTIR spectra of bare SAMNs and SAMN@TA, before and after the laccase immobilization, are shown in Fig. 4. All the spectral profiles present three main vibrations in the 500–700 cm^{-1} region related to the Fe-O stretching arising from the metal oxide lattice, thus confirming the preservation of the maghemite core in SAMN@TA and SAMN@TA@*TvL* hybrids. The broad band between 3000 and 3700 cm^{-1} centred at ~ 3400 cm^{-1} derives from hydroxyl stretching vibrations [43], while the 1640 cm^{-1} band, visible only in pristine SAMNs, is due to adsorbed water on iron oxides and corresponds the H-O-H bending vibration [44,45].

The SAMN@TA hybrid, besides the typical maghemite vibrations, exhibited a series of bands in the 1000–1750 cm^{-1} region,

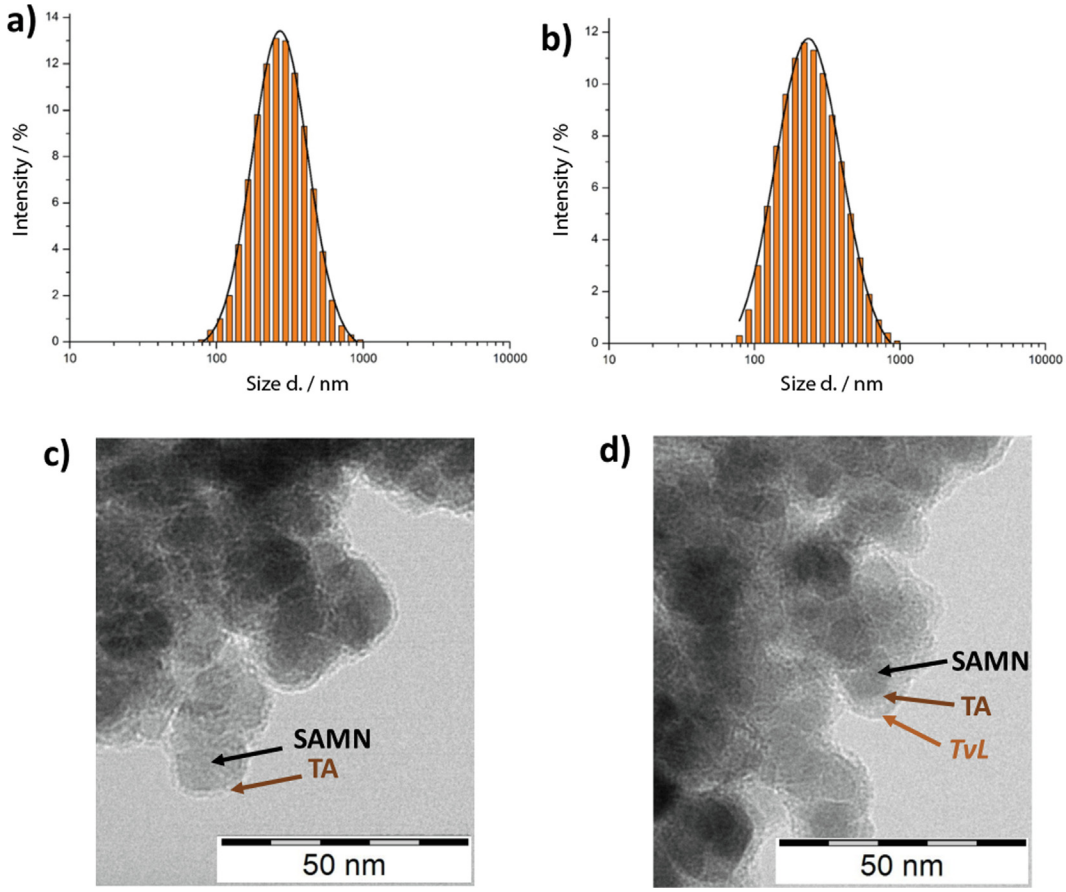

Fig. 3. Characterization of the SAMN@TA and SAMN@TA@*TvL* hybrids by dynamic light scattering (DLS) and transmission electron microscopy (TEM). (a, b) Hydrodynamic size of SAMN@TA (a) and SAMN@TA@*TvL* complex (b) by DLS analysis; (c, d) TEM micrographs of SAMN@TA (c) and SAMN@TA@*TvL* complex (d). The presence of organic shells are visible (see arrows).

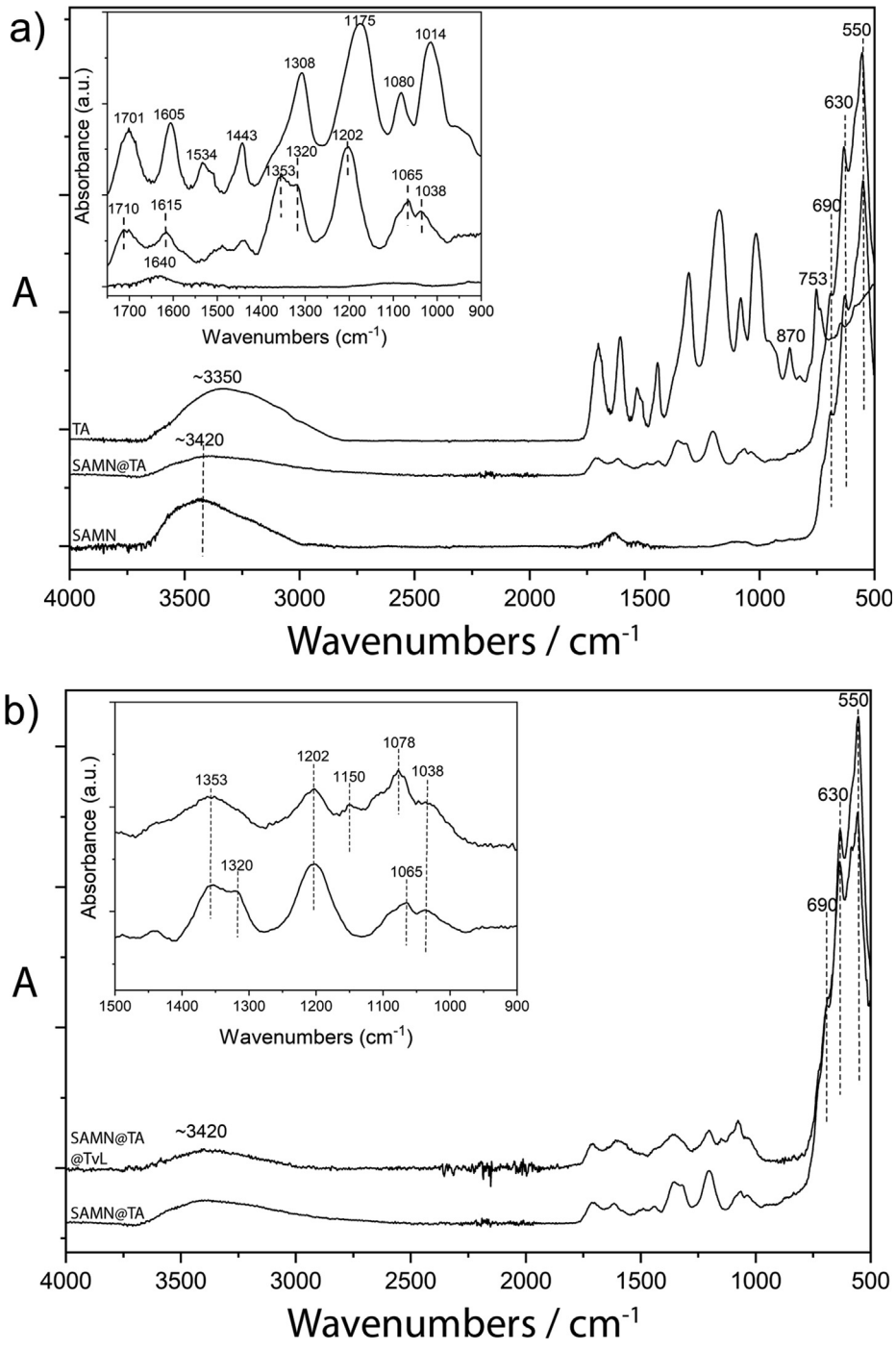

Fig. 4. FTIR spectra of (a) bare SAMNs, SAMN@TA and TA (inset: highlight of the 900–1750 cm^{-1} region) and (b) SAMN@TA and SAMN@TA@*TvL* (inset: highlight of the 900–1500 cm^{-1} region).

plausibly due to the vibrational contributions of the carbonyl and phenolic groups of the ferric tannate layer. Specifically, the 1400–1750 cm^{-1} region is consistent with the presence of the aromatic backbone of pure TA. In particular, the four main vibrational bands can be ascribed as follows: 1701 cm^{-1} to the C═O symmetric stretch [46–48], 1605 cm^{-1} to OH bending vibration [49], and the couple at 1534 and 1443 cm^{-1} to the stretching vibrations of the C═C skeletal ring of aromatic rings [47,50]. The bands at 1100–1300 cm^{-1} can be assigned to C—O stretching vibrations [46-48], while the two small bands at 753 and 870 cm^{-1} to the C═C vibrations of aromatic rings [46,51].

Several IR bands of TA were shifted to higher wavenumbers upon the formation of the SAMN@TA hybrid and vibrational features of carbonyl groups (C═O and C—O) resulted subjected to the most significant variations, indicating their involvement in the interaction with SAMN surface [46,52]. Differently, only minor modifications were observed on hydroxyl groups features. Noteworthy, the C═C vibrations of aromatic rings cannot be identified in the hybrid, evidencing their participation in the interaction with the surface of SAMNs. It is important to recall that the interplay between SAMNs and tannic acid led to a drastic reorganization of the nanoparticle surface leading to the development of a shell

constituted of a complex network of ferric tannates [18]. The present FTIR results substantiated the important role played by C=O and C=C functionalities of TA in the peculiar nanostructured interface.

Notwithstanding most enzyme bands overlapped with the ones of the ferric tannate shell, complicating the punctual identification of single functional group contributions, the comparison of the IR spectra of SAMN@TA before and after the spontaneous binding of laccase showed the appearance of new additional features in the final nano-bioconjugate (Fig. 4b and inset). Firstly, a new IR band at 1150 cm^{-1} due to preserved hydroxyl vibrations of the phenolic group of the enzyme can be observed in the complex [53].

Noteworthy, a slight reorganization of the ferric tannate shell emerged from the analysis of the main IR profile. Besides a band shift from 1065 cm^{-1} to 1078 cm^{-1}, a significant shape modification occurred to a double band falling in the 1300–1400 cm^{-1} region. This feature was characterized by two maxima at 1320 and 1350 cm^{-1} in the parent SAMN@TA spectrum. The enzyme docking led to the disappearance of the vibration at 1320 cm^{-1}, likely due to carbonyl groups of TA, accompanied by the broadening of the component at 1350 cm^{-1}. Intriguingly, such a broadening to higher wavenumbers can be correlated to the combination of C–N in-plane bending of amide I and symmetric C—O stretching of ferric tannates [54].

It should be mentioned that the interaction with a solid surface usually requires a structural adaption of the enzyme and, in the worst situation, this reorganization results in the protein denaturation and to the complete loss of its biological properties [10]. Spectroscopic results suggested that the ferric tannate layer on the nanoparticles could be characterized by plasticity properties. This fascinating facet of the interaction between proteins and tannates may be helpful for minimizing structural modifications of enzymes and, therefore, for containing possible negative impact on catalytic activity. This aspect deserves a deeper investigation and will be object of further studies.

3.2. Kinetic characterization of native TvL and of the SAMN@TA@TvL hybrid

The catalytic activity of *TvL* was characterized with model compounds, as substrates, mimicking natural phenolics, namely 1,2-dihydroxy-benzene, 1,3-dihydroxy-benzene and 1,4-dihydroxy-benzene isomers, as a function of pH (see Supplementary Information). Specifically, oxygraphic measurements were carried out on the three substrates, whereas spectrophotometric determinations were performed on 1,2-dihydroxybenzene and 1,4-dihydroxybenzene. Indeed, this technique was not suitable for 1,3-dihydroxybenzene, as its enzymatic oxidation is not optically detectable as its oxidation product is not a quinone. For further measurements, 1,4-dihydroxybenzene was used as reference substance.

Considering that the maximum catalytic activity of *TvL* was around pH 5.0, 50 mM citrate buffer, pH 5.0, was used as medium buffer for the subsequent experiments. Furthermore, in the view of the final electrochemical biosensor configuration, which require a supporting electrolyte in the buffer solution, and considering that laccases are copper proteins frequently inhibited by inorganic anions [55], enzyme activity on 1,4-hydroquinone as substrate was checked in the presence of different anions in the form of potassium salts. In particular, KCl, $KClO_4$ and KNO_3 were tested. The enzyme was influenced by salt additions and results are summarized in Table S1 (Supporting Information). The enzyme was heavily inhibited by chloride ions as already reported for other copper proteins [55]. Possibly, the effect is due to the binding properties of chloride on copper ions in the enzyme active site [20]. The potassium salt showing the highest catalytic efficiency (k_{cat}/K_m) was KNO_3, and this salt was used as supporting electrolyte for electrochemical measurements (see Table S1 in Supporting Information).

Successively, the enzymatic activity of the SAMN@TA@*TvL* ternary hybrid was studied by spectrophotometry on 1,4-dihydroxybenzene as substrate. Measurements indicated that *TvL* was successfully immobilized on SAMNs, showing a detectable catalytic activity. Moreover, the catalytic activity of the hybrid was compared with that of native *TvL* under the same experimental conditions, and the kinetic parameters were calculated (see Table S2 in Supporting Information). The conjugation of the enzyme with the nanoparticles led to one order of magnitude decrease of the catalytic constant, k_{cat}, while the K_m value was halved. Consequently, the catalytic efficiency, k_{cat}/K_m, decreased of around one order of magnitude with respect to the native enzyme. It should be mentioned that the catalytic activity of SAMN@TA@TvL hybrid was measured under different stirring conditions evidencing that it was not diffusion controlled.

It is generally assumed that immobilization of enzymes can modify the macromolecular structure resulting in a decrease of catalytic constant and the role of structural alterations on the catalytic properties of laccases was excellently reviewed [56]. Possibly, the observed reduction of the catalytic constant, k_{cat}, of the enzyme in the SAMN@TA@*TvL* ternary hybrid (see Table S2 in Supporting Information) can be explained in terms of a modification of the enzyme structure upon immobilization. In fact, in laccases even slight alterations of the copper site geometry can drastically affect the electron transfer rate during substrate oxidation catalysis [56]. Differently, the observed K_m decrease (corresponding to an increase of laccase affinity for the substrate) upon immobilization is quite rare. Nevertheless, it was already reported for the laccase from *Trametes versicolor* and interpreted in terms of an increased suitability of the enzyme active site towards substrate recognition [57].

At the same time, immobilization on a solid support can increase the stability of immobilized enzymes [12]. Indeed, the storage stability of the hybrid, at 4.0° C, was 6 months as checked by monitoring the enzymatic activity by Uv–Vis spectrophotometry.

3.3. Development of a polyphenol biosensor

The SAMN@TA@*TvL* hybrid was used as biological recognition element for the development of a biosensor aimed at the oxidation of phenolic compounds, using a gold working electrode as electrochemical transducer (see Fig. 1). The functioning principle of the biosensor is based on the enzymatic oxidation of polyphenols by the immobilized *TvL* with the concomitant formation of oxidized phenolic species. The electro-reduction of these compounds at the gold electrode completed the detection system.

Firstly, the electrochemical behavior of the gold electrode was studied, using 1,4-hydroquinone (enzyme substrate) and 1,4 benzoquinone (product of enzyme oxidation) as electroactive substances by Square Wave Voltammetry (SWV). The appearance of a concentration dependent SWV peak at around –0.20 V for benzoquinone reduction (see Fig. 5) and at +0.44 V for hydroquinone oxidation (data not shown) witnessed the electrocatalytic behavior of the two organic molecules at the gold working electrode.

The redox behavior of the 1,4-hydroquinone/1,4-benzoquinone redox couple was reconsidered upon modification of the working electrode with SAMN@TA. For this purpose, 4 μL of 500 mg L^{-1} SAMN@TA were deposited on the gold electrode surface and the hybrid was immobilized by means of a magnet positioned on the opposite side of the electrode. Noteworthy, SAMN@TA was able to silence the electrode response toward the 1,4-hydroquinone electro-oxidation, while 1,4-benzoquinone reduction was detected at −0.15 V (see Fig. 5). Interestingly, the nanomaterial layer led to a

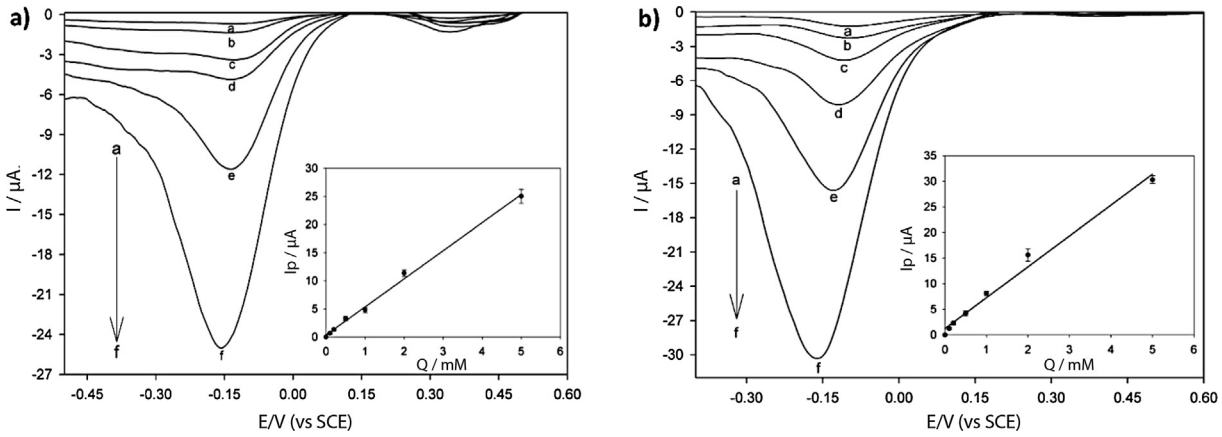

Fig. 5. SWV of 1,4-benzoquinone on unmodified gold electrode (a) and on SAMN@TA modified electrode (b). Insets: The corresponding calibration plots. Measurements were carried out in 50 mM sodium citrate buffer (pH 5.0), containing 50 mM KNO_3 as supporting electrolyte. Experimental SWV parameters were: +0.6 V initial potential, −0.5 V end-point potential, 5 mV potential step, 20 mV amplitude, 25 Hz frequency, 5 s equilibration time, 125 mV s^{-1} scan rate. The concentrations of 1,4-benzoquinone was: (a) 0.1 mM, (b) 0.2 mM, (c) 0.5 mM, (d) 1 mM, (e) 2 mM, (f) 5 mM.

slight improvement of the electrocatalytic performances toward 1,4-benzoquinone reduction with respect to the unmodified electrode. Indeed, under these conditions, the sensitivity resulted 5.0 ± 0.2nA μM^{-1} and 6.0 ± 0.5nA μM^{-1}, and the LOD were 4.2 µM and 3.5 µM for the pristine and the modified gold electrode, respectively (see Fig. 5).

Finally, the gold working electrode surface was functionalized with the SAMN@TA@*TvL* hybrid. The best working conditions were investigated by monitoring the biosensor response as a function of the volume (in the 2–8 µL range) of the nano-bioconjugate suspension (500 mg L^{-1}) used for the depositions on the electrode surface. The best analytical performance was achieved by dropping 4 µL of a 0.5 mg mL^{-1} suspension (corresponding to 46 ng of *TvL*) of the biologically active ternary hybrid, using a permanent magnet for the bioelement immobilization on the electrode.

The electrochemical system responded to the additions of 1,4-hydroquinone at −0.2 V, evidencing the production of 1,4-benzoquinone by the catalytic activity of immobilized laccase. The peak current intensity linearly increased in the 0.1–10 µM 1,4-hydroquinone concentration range (see Fig. 6).

These results, confirmed the efficient production of 1,4-benzoquinone by the immobilized laccase and its reduction at the working electrode at a relatively low applied potential. The sensitivity of the electrode modified with SAMN@TA@*TvL*, with respect to hydroquinone, was 868.9 ± 1.9nA μM^{-1}, and the LOD was 81 nM. Moreover, the reproducibility of the biosensor was evaluated and resulted of about 5.0% on 5 different modified electrodes. Therefore, in consideration of the building immediacy, cost effectiveness and analytical performances, the proposed biosensor represents an interesting option among analogue systems available in literature (see Table 1).

3.4. Application of SAMN@TA@TvL for the electrochemical determination of polyphenols in real samples (blueberry extracts)

The gold/SAMN@TA@*TvL* electrode was used to determine polyphenols in real samples (blueberry extracts) by square wave

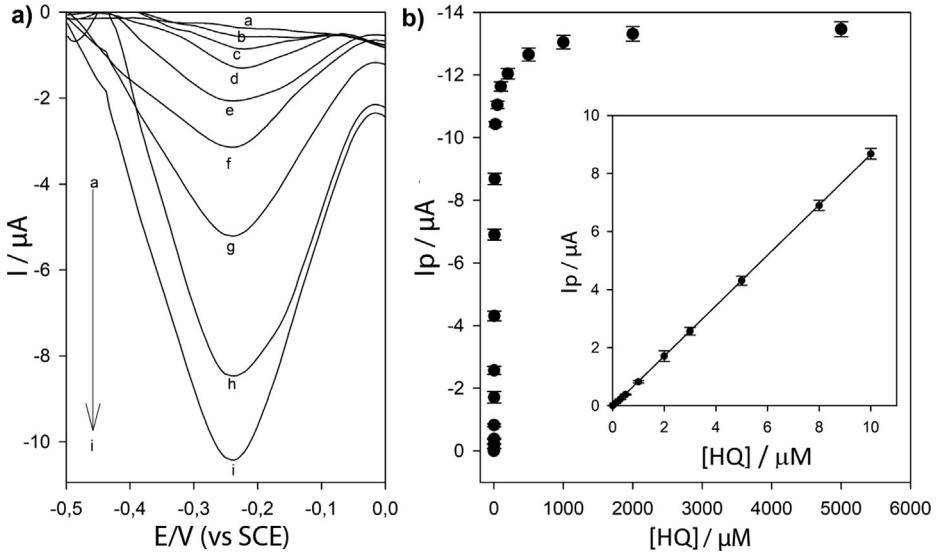

Fig. 6. Response of the SAMN@TA@*TvL* modified gold electrode. (a) SWV of 1,4-hydroquinone addition on the SAMN@TA@*TvL* modified gold electrode. The concentrations of 1,4-hydroquinone was (a) 0.1 µM, (b) 0.3 µM, (c) 0.5 µM, (d) 1 µM, (e) 2 µM, (f) 3 µM, (g) 5 µM, (h) 8 µM, (i) 10 µM; (b) Pseudo-Michaelis-Menten curve obtained by testing the biosensor response in a wide substrate concentration range (0.1–5.0 mM). **Inset**: Calibration plot. Measurements were carried out in 50 mM sodium citrate buffer (pH 5.0), containing 50 mM KNO_3 as supporting electrolyte. Experimental SWV parameters were: +0.6 V initial potential, −0.5 V end-point potential, 5 mV potential step, 20 mV amplitude, 25 Hz frequency, 5 s equilibration time, 125 mV s^{-1} scan rate.

Table 1
Comparison of the sensing performances of different electrochemical biosensors based on *TvL* for polyphenol detection.

Electrode assembly	Electrode surface	Analytical technique	Detection limit (nM)	Linear range (μM)	Sensitivity (μA nM^{-1})	Ref.
bacterial cellulose – Au nanoparticles	GCE	DPV	5.71	0.03–0.1	0.3029	[58]
NiCu alloy nanoparticle - carbon nanofibers	GCE	LSV	90	0.4–2.37	1.5	[59]
Graphene-chitosan composite film	GCE	CA	260	20–100	7.066	[60]
ZnO loaded carbon nanofibers	GCE	SWV	9.5	0.5–2.06	28.5	[61]
Fe_3O_4-SiO_2 nanoparticles	CPE	CA	15	0.1–137.5	0.2118	[62]
Multi-walled carbon nanotube	GCE	CA	600	2–1000	0.0177	[63]
Sol-gel 3D polymer (MPTS)	Au	CA	250	0.9–20	2.84	[64]
PVA-AWP	SPE	CA	1070	1.1–130	9.44	[65]
Graphene-cellulose microfibers (GR-CMF)	SPCE	CV	85	0.2–209.7	0.932	[66]
SAMN@TA	Au	SWV	81	0.1–10	0.87	This work

Note: Au, gold electrode; CA, chronoamperometry; CPE, carbon paste electrode; CV, cyclic voltammetry; DPV, differential pulse voltammetry; GCE, glassy carbon electrode; LSV, linear sweep voltammetry; MPTS, (3-mercaptopropyl)-trimethoxysilane; PVA-AWP, polyvinyl alcohol-azide-unit pendant water-soluble photopolymer; SPCE, screen printed carbon electrode SPE, screen printed electrode; SWV, square wave voltammetry.
Note: Au, gold electrode; CA, chronoamperometry; CPE, carbon paste electrode; CV, cyclic voltammetry; DPV, differential pulse voltammetry; GCE, glassy carbon electrode; LSV, linear sweep voltammetry; MPTS, (3-mercaptopropyl)-trimethoxysilane; PVA-AWP, polyvinyl alcohol-azide-unit pendant water-soluble photopolymer; SPCE, screen printed carbon electrode SPE, screen printed electrode; SWV, square wave voltammetry.

voltammetry. The sample was diluted 1 to 200 for the measurements and the polyphenol concentration in the real samples was 1.26 ± 0.55 mM, expressed as hydroquinone equivalents.

The polyphenol content in the blueberry extract was compared with measurements by conventional methods, such as the ferric reducing antioxidant power (FRAP) [35], the Folin-Ciocalteu method [36] and by HPLC as described in the Experimental Section (see Table 2).

Differences among the polyphenol determination methods are evident in Table 2. It should be considered that conventional methods used in the present study to assess the polyphenol content in real samples follow complex oxidation reactions. Moreover, the composition of plant products is very complex and many antioxidant compounds besides polyphenols, spanning from vitamins to thiol containing substances, with possible synergistic interactions, can be found. Indeed, the number of methods used to measure polyphenols in reals samples is over one hundred, even if no validated assay was universally accepted, and several reviews have been published on this topic expressing variable opinions [67,68]. According to the reaction mechanism of the method used, different side-reactions may perturb the obtained values. In the present study, FRAP method and the Folin-Ciocalteu reagent were applied for measuring the total polyphenolic content in samples. Both methods are based on the measurement of electron transfer reactions, and are not selective for polyphenolic components [69]. For comparison, HPLC measurements were carried out. In this case, the difference with respect to the biosensor can be attributed to the fact that chromatographic measurements revealed only known polyphenolic substances with commercially available standards, while *TvL* presents a very low substrate specificity, thus catalyzing the oxidation of a wider polyphenol spectrum [70].

Finally, the stability of the biosensor response was tested for 9 h per day and storing overnight at 4 °C. Under these operative conditions, the response of the biosensor was stable for 6 months.

Table 2
Measurement of the polyphenol content in blueberry extract by different methods.

Method	Polyphenol content (mM)
FRAP	8.70 ± 2.20
Folin-Chocalteau	0.42 ± 0.04
HPLC	0.46 ± 0.01
Biosensor	1.26 ± 0.55

4. Conclusions

In the present work, a functional core-shell hybrid nanoparticle was developed (SAMN@TA). The maghemite core conferred magnetic drivability to SAMN@TA, while reactive ferric tannates constituting the shell, thanks to the chemical properties endowed by parent TA, offered a versatile surface for anchoring biologically active macromolecules. In this view, the suitability of the TA coating on magnetic nanoparticles as docking surface was demonstrated using *TvL* as a model enzyme, and a new enzymatic active nano-bioconjugate (SAMN@TA@*TvL*) was successfully prepared by self-assembly in water. The SAMN@TA@*TvL* ternary hybrid was employed to develop an electrochemical biosensor by its simple magnetic immobilization on a gold electrode (gold/SAMN@TA@*TvL*) and used for polyphenols biosensing. Previously, catalytic parameters of the native enzyme were studied in order to optimize the biosensor response, and the proposed system was able to detect polyphenols with a sensitivity of 868.9 ± 1.9nA μM^{-1} and a detection limit of 81 nM.

The biosensor here presented, coupling cost effectiveness and fabrication simplicity to good analytical performances, represents a valid option in comparison to analogue biosensor designs available in literature.

Thanks to the low substrate specificity and the high activity of the laccase from *Trametes versicolor*, the proposed biosensor can be potentially used for the detection of polyphenols in a large number real samples. However, the advantages of SAMN@TA are of general interest and the proclivity of TA to interact with proteins suggests that SAMN@TA can be proposed as a versatile solution for the direct immobilization of enzymes and for the construction of novel electrochemical sensing platforms.

Declaration of Competing Interest

The authors declared that there is no conflict of interest.

Acknowledgments

This work was supported by the Veneto Region project "Safe, Smart, Sustainable Food for Health (3S_4H)"- POR FESR 2014-2020, 1.1.4. DGR n. 1139, the Cariparo Foundation (Padova and Rovigo, Italy), DOR funds of the University of Padova (DOR1989373, Fabio Vianello) and the excellence department project of the Italian Ministry of Education, University and research (MIUR) "Excellence for Aquatic Animal Health - ECCE AQUA".

Authors thank Tectronik s.r.l (Padua, Italy) for providing the gold electrodes.

Appendix A. Supplementary material

Supplementary data to this article can be found online at https://doi.org/10.1016/j.bioelechem.2019.107418.

References

[1] A.N. Kozitsina, T.S. Svalova, N.N. Malysheva, A.V. Okhokhonin, M.B. Vidrevich, K.Z. Brainina, Sensors based on bio and biomimetic receptors in medical diagnostic, environment, and food analysis, Biosensors 8 (2018) 35, https://doi.org/10.3390/bios8020035.

[2] V. Urbanova, M. Magro, A. Gedanken, D. Baratella, F. Vianello, R. Zboril, Nanocrystalline iron oxides, composites, and related materials as a platform for electrochemical, magnetic, and chemical biosensors, Chem. Mater. 26 (2014) 6653–6673, https://doi.org/10.1021/cm500364x.

[3] B.M. Brena, F. Batista-Viera, Immobilization of enzymes, in: J.M. Guisan (Ed.), Immobilization of Enzymes and Cells, Humana Press, New Jersey, 2006.

[4] J. Garcia, Y. Zhang, H. Taylor, O. Cespedes, M.E. Webb, D. Zhou, Multilayer enzyme-coupled magnetic nanoparticles as efficient, reusable biocatalysts and biosensors, Nanoscale 3 (2011) 3721–3730, https://doi.org/10.1039/C1NR10411J.

[5] K. Niemirowicz, K.H. Markiewicz, A.Z. Wilczewska, H. Car, Magnetic nanoparticles as new diagnostic tools in medicine, Adv. Med. Sci. 57 (2012) 196–207, https://doi.org/10.2478/v10039-012-0031-9.

[6] M. Mahmoudi, N. Bertrand, H. Zope, O.C. Farokzad, Emerging understanding of the protein corona at the nano-bio interfaces, Nano Today 11 (2016) 817–832, https://doi.org/10.1016/j.nantod.2016.10.005.

[7] K.A. Johnson, Role of induced fit in enzyme specificity: a molecular forward/reverse switch, J. Biol. Chem. 283 (2008) 26297–26301, https://doi.org/10.1074/jbc.R800034200.

[8] A.S.M. Chong, X.S. Zhao, Design of large-pore mesoporous materials for immobilization of penicillin G acylase biocatalyst, Catal. Today 93–95 (2004) 293–299, https://doi.org/10.1016/j.cattod.2004.06.064.

[9] C. Pan, B. Hu, W. Li, Y. Sun, H. Ye, X. Zeng, Novel and efficient method for immobilization and stabilization of β-D-galactosidase by covalent attachment onto magnetic Fe_3O_4–chitosan nanoparticles, J. Mol. Catal. B Enz. 61 (2009) 208–215, https://doi.org/10.1016/j.molcatb.2009.07.003.

[10] I. Lynch, K.A. Dawson, Protein-nanoparticle interactions, Nano Today 3 (2008) 40–47, https://doi.org/10.1016/S1748-0132(08)70014-8.

[11] S. Rana, Y.C. Yeh, V.M. Rotello, Engineering the nanoparticle-protein interface: applications and possibilities, Curr. Opin. Chem. Biol. 14 (2010) 828–834, https://doi.org/10.1016/j.cbpa.2010.10.001.

[12] M. Misson, H. Zhang, B. Jin, Nanobiocatalyst advancements and bioprocessing applications, J. R. Soc. Interface 12 (2015) 20140891, https://doi.org/10.1098/rsif.2014.0891.

[13] M. Martín, P. Salazar, R. Villalonga, S. Campuzano, J.M. Pingarrón, J.L. González-Mora, Preparation of core–shell Fe_3O_4@poly(dopamine) magnetic nanoparticles for biosensor construction, J. Mater. Chem. B 2 (2014) 739–746, https://doi.org/10.1039/C3TB21171A.

[14] M. Magro, D. Baratella, G. Miotto, J. Frömmel, M. Šebela, M. Kopečná, E. Agostinelli, F. Vianello, Enzyme self-assembly on naked iron oxide nanoparticles for aminoaldehyde biosensing, Amino Acids 51 (2019) 679–690, https://doi.org/10.1007/s00726-019-02704-7.

[15] D. Baratella, M. Magro, G. Sinigaglia, R. Zboril, G. Salviulo, F. Vianello, A glucose biosensor based on surface active maghemite nanoparticles, Biosens. Bioelectron. 45 (2013) 13–18, https://doi.org/10.1016/j.bios.2013.01.043.

[16] T.S. Sileika, D.G. Barrett, R. Zhang, K.H.A. Lau, P.B. Messersmith, Colorless multifunctional coatings inspired by polyphenols found in tea, chocolate, and wine, Angew. Chem. 52 (41) (2013) 10766–10770, https://doi.org/10.1002/anie.201304922.

[17] J. de Almeida Roger, M. Magro, S. Spagnolo, E. Bonaiuto, D. Baratella, L. Fasolato, F. Vianello, Antimicrobial and magnetically removable tannic acid nanocarrier: a processing aid for Listeria monocytogenes treatment for food industry applications, Food Chem. 267 (2018) 430–436, https://doi.org/10.1016/j.foodchem.2017.06.109.

[18] M. Magro, E. Bonaiuto, D. Baratella, J. de Almeida Roger, P. Jakubec, V. Corraducci, J. Tuček, O. Malina, R. Zbořil, F. Vianello, Electrocatalytic nanostructured ferric tannates: characterization and application of a polyphenol nanosensor, ChemPhysChem 17 3196–3203 (2016), https://doi.org/10.1002/cphc.201600718.

[19] G.J. Davies, V. Ducros, V. Laccases, Handbook of Metalloproteins, John Wiley & Sons, Chichester, 2001, pp. 1359–1368.

[20] F. Xu, Oxidation of phenols, anilines and benzenethiols by fungal laccases: Correlation between activity and redox potentials as well as halide inhibition, Biochem. 35 (1996) 7608–7614, https://doi.org/10.1021/bi952971a.

[21] E.I. Solomon, U.M. Sundaram, T.E. Machonkin, Multicopper oxidases and oxygenases, Chem. Rev. 96 (1996) 2563–2605, https://doi.org/10.1021/cr950046o.

[22] N. Duran, M.A. Rosa, A. D'Annibale, L. Gianfreda, Applications of laccase and tyrosinases (phenoloxidases) immobilised on different supports: a review, Enzyme Microb. Technol. 31 (2002) 907–931, https://doi.org/10.1016/S0141-0229(02)00214-4.

[23] J.M. Bollag, A. Leonowicz, Comparative studies of extracellular fungal laccases, Appl. Environ. Microbiol. 48 (1984) 849–854.

[24] D.S. Arora, P.K. Gill, Laccase production by some white rot fungi under different nutritional conditions, Biores. Technol. 73 (2000) 283–285, https://doi.org/10.1016/S0960-8524(99)00141-8.

[25] R.S. Freire, N. Duran, L.T. Kubota, Development of a laccase-based flow injection electrochemical biosensor for the determination of phenolic compounds and its application for monitoring remediation of Kraft E1 paper mill effluent, Anal. Chim. Acta 463 (2002) 229–238, https://doi.org/10.1016/S0003-2670(02)00417-8.

[26] B. Haghighi, L. Gorton, T. Rutzgas, L.J. Jonsson, Characterization of graphite electrodes modified with laccase from Trametes versicolor and their use for bioelectrochemical monitoring of phenolic compounds in flow injection analysis, Anal. Chim. Acta 487 (2003) 3–14, https://doi.org/10.1016/S0003-2670(03)00077-1.

[27] J. Kulys, R. Vidziunaite, Amperometric biosensor based on recombinant laccases for phenols determination, Biosens. Bioelectron. 18 (2003) 319–325, https://doi.org/10.1016/S0956-5663(02)00172-0.

[28] D. Quan, Y. Kim, W. Shin, Characterization of an amperometric laccase electrode covalently immobilized on platinum surface, J. Electroanal. Chem. 561 (2004) 181–189, https://doi.org/10.1016/j.jelechem.2003.08.003.

[29] A. Makower, A.V. Eremenko, K. Streffer, U. Wollenberg, F.W. Scheller, Tyrosinase-glucose dehydrogenase substrate-recycling biosensor: a highly sensitive measurements of phenolic compounds, J. Chem. Tech. Biotechnol. 65 (1996) 39–44, https://doi.org/10.1002/(SICI)1097-4660(199601)65:1<39::AID-JCTB377>3.0.CO;2-Q.

[30] M. Hedemno, A. Narvaez, E. Dominguez, I. Katakis, Improved mediated tyrosinase amperometric enzyme electrodes, J. Electroanal. Chem. 425 (1997) 1–11, https://doi.org/10.1016/S0022-0728(96)04966-2.

[31] A.K. Singh, R. Chandra, Pollutants released from the pulp paper industry: Aquatic toxicity and their health hazards, Aquat. Toxicol. 211 (2019) 202–216, https://doi.org/10.1016/j.aquatox.2019.04.007.

[32] J. Michałowicz, W. Duda, Phenols – sources and toxicity, Pol. J. Environ. Stud. 16 (2007) 347–362.

[33] A. Kumar, A.K. Mishra, Biological importance of phenol derivatives as potent bioactive compound: a review, Lett. Org. Chem. 15 (2018) 251–264, https://doi.org/10.2174/1570178614666171130155539.

[34] J.K. Kibet, H. Bemmadji, R. Asatryan, L. Khachatryan, Health and environmental impacts of phenols: The role of radicals, in: M. Rutherford (Ed.), Free Radicals and Health, Nova Science, New York, 2016, pp. 1–40.

[35] I.F.F. Benzie, J.J. Strain, The ferric reducing ability of plasma (FRAP) as a measure of "antioxidant power": the FRAP assay, Anal. Biochem. 239 (1996) 70–76, https://doi.org/10.1006/abio.1996.0292.

[36] A. Cano, J. Hernández-Ruíz, F. García-Cánovas, M. Acosta, M.B. Arnao, An end-point method for estimation of the total antioxidant activity in plant material, Phytochem. Anal. 9 (1998) 196–202, https://doi.org/10.1002/(SICI)1099-1565(199807/08)9:4<196::AID-PCA395>3.0.CO;2-W.

[37] V.S. Stoll, J.S. Blanchard, Buffers: principles and practice, Methods Enzymol. 182 (1990) 24–38, https://doi.org/10.1016/0076-6879(90)82006-N.

[38] M.M. Bradford, A rapid and sensitive method for the quantitation of proteins utilizing the principle of protein-dye binding, Anal. Biochem. 72 (1976) 248–254, https://doi.org/10.1016/0003-2697(76)90527-3.

[39] Ann E. Hagerman, Chemistry of Tannin-Protein Complexation, in: Richard W. Hemingway, Joseph J. Karchesy, Susan J. Branham (Eds.), Chemistry and Significance of Condensed Tannins, Springer US, Boston, MA, 1989, pp. 323–333.

[40] C. Pfeiffer, C. Rehbock, D. Hühn, C. Carrillo-Carrion, D.J. de Aberasturi, V. Merk, S. Barcikowski, W.J. Parak, Interaction of colloidal nanoparticles with their local environment: the (ionic) nanoenvironment around nanoparticles is different from bulk and determines the physico-chemical properties of the nanoparticles, J. R. Soc. Interface 11 (96) (2014) 20130931, https://doi.org/10.1098/rsif.2013.0931.

[41] J.N. Miller, J.C. Miller, Statistics and Chemometrics for Analytical Chemistry, Pearson, Harlow, 2010.

[42] V.R. Patel, Y.K. Agrawal, Nanosuspension: an approach to enhance solubility of drugs, J. Adv. Pharm. Technol. Res. 2 (2011) 81–87, https://doi.org/10.4103/2231-4040.82950.

[43] H. Namduri, S. Nasrazadani, Quantitative analysis of iron oxides using Fourier transform infrared spectrophotometry, Corros. Sci. 50 (2008) 2493–2497, https://doi.org/10.1016/j.corsci.2008.06.034.

[44] J.D. Russell, Infrared spectroscopy of ferrihydrite: evidence for the presence of structural hydroxyl groups, Clay Miner. 14 (2) (1979) 109–114, https://doi.org/10.1180/claymin.1979.014.2.03.

[45] D. Walter, Characterization of synthetic hydrous hematite pigments, Thermochim Acta 445 (2) (2006) 195–199, https://doi.org/10.1016/j.tca.2005.08.011.

[46] B. Stuart, S. Preface, Infrared Spectroscopy: Fundamentals and Applications, John Wiley & Sons, Chichester, 2004.

[47] M. Pantoja-Castro, H. González-Rodríguez, Study by infrared spectroscopy and thermogravimetric analysis of tannins and tannic acid, Rev. Latinoam. Quím. 39 (2011) 107–112.

[48] Y.M. Li, X. Miao, Z.G. Wei, J. Cui, S.Y. Li, R.M. Han, Y. Zhang, W. Wei, Iron-tannic acid nanocomplexes: facile synthesis and application for removal of methylene blue from aqueous solution, Dig. J. Nanomater. Bios. 11 (2016) 1045–1061.
[49] M. Božič, S. Gorgieva, V. Kokol, Homogeneous and heterogeneous methods for laccase-mediated functionalization of chitosan by tannic acid and quercetin, Carbohydr. Polym. 89 (3) (2012) 854–864, https://doi.org/10.1016/j.carbpol.2012.04.021.
[50] M. Jastrzebska, J. Zalewska-Rejdak, R. Wrzalik, A. Kocot, I. Mroz, B. Barwinski, B. Cwalina, Tannic acid-stabilized pericardium tissue: IR spectroscopy, atomic force microscopy, and dielectric spectroscopy investigations, J. Biomed. Mat. Res. A 78 (2006) 148–156, https://doi.org/10.1002/jbm.a.30717.
[51] G. Socrates, Infrared and Raman Characteristic Group Frequencies. Tables and Charts, John Wiley & Sons, Chichester, 2004.
[52] K. Rajar, R.A. Soomro, Z.H. Ibupoto, A. Balouch Sirajuddin, Tannic acid assisted copper oxide nanoglobules for sensitive electrochemical detection of bisphenol A, Int. J. Food Prop. 20 (2017) 1359–1367, https://doi.org/10.1080/10942912.2016.1209776.
[53] A.I. El-Batal, N.M. Elkenawy, A.S. Yassin, M.A. Amin, Laccase production by Pleurotus ostreatus and its application in synthesis of gold nanoparticles, Biotechnol. Rep. 5 (2015) 31–39, https://doi.org/10.1016/j.btre.2014.11.001.
[54] D. Alba-Molina, D. Rodríguez-Padrón, A.R. Puente-Santiago, J.J. Giner-Casares, M.T. Martín-Romero, L. Camacho, R. Luque, Mimicking the bioelectrocatalytic function of recombinant CotA laccase through electrostatically self-assembled bioconjugates, Nanoscale 11 (2019) 1549–1554, https://doi.org/10.1039/C8NR06001K.
[55] O.V. Morozova, G.P. Shumakovich, M.A. Gorbacheva, S.V. Shleev, A.I. Yaropolov, "Blue" laccases, Biochemistry (Mosc.) 72 (2007) 1136–1150, https://doi.org/10.1134/S0006297907100112.
[56] S.M. Jones, E.I. Solomon, Electron transfer and reaction mechanism of laccases, Cell. Mol. Life Sci. 72 (2015) 869–883, https://doi.org/10.1007/s00018-014-1826-6.
[57] Martina Vršanská, Stanislava Voběrková, Ana Jiménez Jiménez, Vladislav Strmiska, Vojtěch Adam, Preparation and optimisation of cross-linked enzyme aggregates using native isolate white rot fungi trametes versicolor and fomes fomentarius for the decolourisation of synthetic dyes, IJERPH 15 (1) (2017) 23, https://doi.org/10.3390/ijerph15010023.
[58] G. Li, K. Sun, D. Li, P. Lv, Q. Wang, F. Huang, Q. Wei, Biosensor based on bacterial cellulose-Au nanoparticles electrode modified with laccase for hydroquinone detection, Colloids Surf. A Physicochem. Eng. Asp. 509 (2016) 408–414, https://doi.org/10.1016/j.colsurfa.2016.09.028.
[59] D. Li, P. Lv, J. Zhu, Y. Lu, C. Chen, X. Zhang, Q. Wei, NiCu alloy nanoparticle-loaded carbon nanofibers for phenolic biosensor applications, Sensors 15 (2015) 29419–29433, https://doi.org/10.3390/s151129419.
[60] J. Qu, T. Lou, S. Kang, X. Du, Laccase biosensor based on graphene-chitosan composite film for determination of hydroquinone, Anal. Lett. 47 (2014) 1564–1578, https://doi.org/10.1080/00032719.2013.867499.
[61] D. Li, J. Yang, J. Zhou, Q. Wei, F. Huang, Direct electrochemistry of laccase and a hydroquinone biosensing application employing ZnO loaded carbon nanofibers, RSC Adv. 4 (2014) 61831–61840, https://doi.org/10.1039/c4ra11469h.
[62] Y. Zhang, G.-M. Zeng, L. Tang, D.-L. Huang, X.-Y. Jiang, Y.-N. Chen, A hydroquinone biosensor using modified core–shell magnetic nanoparticles supported on carbon paste electrode, Biosens. Bioelectron. 22 (2007) 2121–2126, https://doi.org/10.1016/j.bios.2006.09.030.
[63] J. Qu, T. Lou, S. Kang, X. Du, Simultaneous determination of catechol and hydroquinone using a self-assembled laccase biosensor based on nanofilm, Sens. Lett. 11 (2013) 1567–1572, https://doi.org/10.1166/sl.2013.3017.
[64] E. Casero, M.D. Petit-Dominquez, L. Vazquez, I. Ramirez-Asperilla, A.M. Parra-Alfambra, F. Pariente, E. Lorenzo, Laccase biosensors based on different enzyme immobilization strategies for phenolic compounds determination, Talanta 115 (2013) 401–408, https://doi.org/10.1016/j.talanta.2013.05.045.
[65] P. Ibarra-Escutia, J.J. Gomez, C. Calas-Blanchard, J.L. Marty, M.T. Ramirez-Silva, Amperometric biosensor based on a high resolution photopolymer deposited onto a screen-printed electrode for phenolic compounds monitoring in tea infusions, Talanta 81 (2010) 1636–1642, https://doi.org/10.1016/j.talanta.2010.03.017.
[66] S. Palanisamy, S.K. Ramaraj, S.M. Chen, T.C. Yang, P. Yi-Fan, T.W. Chen, V. Velusamy, S. Selvam, A novel laccase biosensor based on laccase immobilized graphene-cellulose microfiber composite modified screen-printed carbon electrode for sensitive determination of catechol, Sci. Rep. 7 (2017) 41214, https://doi.org/10.1038/srep41214.
[67] A.V. Badarinath, K. Mallikarjuna RAo, C. Madhu Sudhana Chetty, S. Ramkanth, T.V.S. Rajan, K. Gnanaprakash, A review on in-vitro antioxidant methods: comparisons, correlations and considerations, Int. J. Pharm. Tech. Res. 2 (2010) 1276–1285.
[68] A. Racz, N. Papp, E. Balogh, M. Fodor, K. Heberger, Comparison of antioxidant capacity assays with chemometric methods, Anal. Methods 7 (2015) 4216–4224, https://doi.org/10.1039/C5AY00330J.
[69] R. Apak, K. Guclu, B. Demirata, M. Ozyurek, S.E. Çelik, B. Bektasoglu, K.I. Berker, D. Ozyurt, Comparative evaluation of various total antioxidant capacity assays applied to phenolic compounds with the CUPRAC assay, Molecules 12 (2007) 1496–1547, https://doi.org/10.3390/12071496.
[70] R. Mehra, J. Muschiol, A.S. Meyer, K.P. Kepp, A structural-chemical explanation of fungal laccase activity, Sci. Rep. 8 (2018) 17285, https://doi.org/10.1038/s41598-018-35633-8.